The patterns in shifts in the shielding tensor elements upon heteroatom substitution or on going from doubly to triply bonded arrangements have been rationalized with very qualitative ideas about chemical shifts. While high-level ab initio calculations now accurately reproduce experimentally observed chemical shifts, such calculations have not as yet produced a great deal of insight into the factors determining chemical shifts. An in-depth exposition of the electronic factors responsible for these shifts and an explanation at an ab initio level for the success of the shift scaling procedure used here then remain as challenging problems for electronic structure theorists. It is expected that development of an understanding at the ab initio level of the trends in tensorial shifts noted in work of the type presented here will be useful in developing better insight from these electronic structure calculations.

Acknowledgment. Support of this work by a grant from the National Science Foundation (CHE-8517584) is gratefully acknowledged. Portions of this work carried out at the University of Texas at Austin were supported by a grant from the National Science Foundation (CHE-8506029) and the Robert A. Welch Foundation. J.C.D. acknowledges support by a graduate fellowship from the Heyl Foundation. K.W.Z. acknowledges stimulating discussions with Prof. C. J. Jameson.

Resonance Raman Pursuit of the Change from Fe^{II}–O_2 to Fe^{III}–OH via Fe^{IV}=O in the Autoxidation of Ferrous Iron–Porphyrin

Y. Mizutani,[1a,b] S. Hashimoto,[1a,c] Y. Tatsuno,[1d] and T. Kitagawa*,[1a,b]

Contribution from the Institute for Molecular Science, Okazaki National Research Institutes, and Department of Functional Molecular Science, School of Mathematical and Physical Science, The Graduate University for Advanced Studies, Myodaiji, Okazaki, 444 Japan, and Faculty of Engineering Science, Osaka University, Toyonaka, Osaka, 565 Japan. *Received February 6, 1990*

Abstract: Resonance Raman (RR) and visible absorption spectra were observed for autoxidation intermediates of ferrous tetramesitylporphyrin [(TMP)Fe^{II}] to the ferric hydroxy derivative [(TMP)Fe^{III}OH] via (TMP)$Fe^{II}O_2$, (TMP)$Fe^{III}OOFe^{III}$(TMP), and (TMP)Fe^{IV}=O. The O–O stretching [$\nu(O_2)$] and Fe^{II}–O_2 stretching [$\nu(Fe^{II}–O_2)$] Raman bands were simultaneously observed at 1171 and 522 cm^{-1}, respectively, for the (TMP)$Fe^{II}O_2$ in toluene solution at −100 °C for the first time. The present data together with the reported IR data for the solution samples indicate a linear inverse correlation between $\nu(O_2)$ and $\nu(Fe^{II}–O_2)$ frequencies similar to that between ν(CO) and $\nu(Fe^{II}–CO)$, but the data from heme proteins fall off the line. Upon raising the sample temperature to −70 °C, formation of (TMP)$Fe^{III}OOFe^{III}$(TMP) was confirmed by ^1H NMR and its visible absorption spectrum was determined. However the peroxo-bridged dimer was so photolabile that it was decomposed into (TMP)Fe^{IV}=O by laser illumination even at −70 °C, and therefore, no oxygen isotope sensitive RR band assignable to (TMP)$Fe^{III}OOFe^{III}$(TMP) was identified. (TMP)Fe^{IV}=O was also photolabile and yielded the photoproduct, the same as the case of thermal decomposition, but (TMP)Fe^{IV}=O gave the Fe^{IV}=O stretching [$\nu(Fe^{IV}=O)$] Raman band at 843 cm^{-1}, which is in agreement with the value reported for the five-coordinate oxoferryl complex. The reduction rate of (TMP)Fe^{IV}=O to (TMP)Fe^{III}OH was different between the toluene-h_8 and -d_8 solutions, suggesting that it proceeds via hydrogen abstraction from toluene. Presumably, the Fe^{IV}=O bond has a partial radical character, which increases upon electronic excitation, and this is the reason why decomposition of (TMP)Fe^{IV}=O is accelerated by laser illumination.

A mechanism of dioxygen activation by iron(II) porphyrin has attracted chemists' attention in relation to elucidation of the catalytic mechanism of various heme enzymes.[2a,b] The presence of the oxy ferrous form ($PFe^{II}O_2$; P denotes a porphyrin dianion) was revealed spectroscopically for cytochrome P-450[3a-c] and cytochrome oxidase[4a-c] as well as for hemoglobin (Hb) and myoglobin (Mb), although structures of the successive reaction intermediates such as the oxoferryl form (PFe^{IV}=O) have not been well documented yet. Physicochemical properties of PFe^{IV}=O in peroxidases have been extensively investigated with Mössbauer,[5a-c] NMR,[6] ENDOR,[7] EXAFS,[8] and resonance Raman (RR) techniques[9a-f] and are compared with those of model

(1) (a) Institute for Molecular Science. (b) Graduate University for Advanced Studies. (c) Present address: Faculty of Pharmaceutical Science, Tohoku University, Aobayama, Sendai, 980 Japan. (d) Osaka University.

(2) (a) Collman, J. P.; Halpert, T. R.; Suslick, K. S. In *Metal Ion Activation of Dioxygen*; Spiro, T. G., Ed.; Wiley: New York, 1980; pp 1-72. (b) Groves, J. T. In *Cytochrome P-450: Structure and Biochemistry*; Ortiz de Montellano, P., Ed.; Plenum Press: New York, 1986; Chapter 1.

(3) (a) Ishimura, Y.; Ullrich, V.; Peterson, J. A. *Biochem. Biophys. Res. Commun.* **1971**, *42*, 140-146. (b) Peterson, J. A.; Ishimura, Y.; Griffin, B. W. *Arch. Biochem. Biophys.* **1972**, *149*, 197-208. (c) Bangcharoenpaurpong, O.; Rizos, A. K.; Champion, P. M. *J. Biol. Chem.* **1986**, *261*, 8089-8092.

(4) (a) Chance, B.; Saronio, C.; Leigh, J. S., Jr. *J. Biol. Chem.* **1975**, *250*, 9226-9237. (b) Varotsis, C.; Woodruff, W. H.; Babcock, G. T. *J. Am. Chem. Soc.* **1989**, *111*, 6439-6440. (c) Orii, Y. *Ann. N.Y. Acad. Sci.* **1988**, *550*, 105-117.

(5) (a) Maeda, Y.; Morita, Y. *Biochem. Biophys. Res. Commun.* **1967**, *29*, 680-685. (b) Moss, T. H.; Ehrenberg, A.; Bearden, A. J. *Biochemistry* **1969**, *8*, 4159-4162. (c) Harami, T.; Maeda, Y.; Morita, Y.; Trautwein, A.; Gonser, U. *J. Chem. Phys.* **1977**, *67*, 1164-1169.

(6) La Mar, G. N.; deRopp, J. S.; Latos-Grazynski, L.; Balch, A. L.; Johnson, R. B.; Smith, K. M.; Parish, D. W.; Cheng, R.-J. *J. Am. Chem. Soc.* **1983**, *105*, 782-787.

(7) Roberts, J. E.; Hoffman, B. M.; Rutter, R.; Hager, L. P. *J. Am. Chem. Soc.* **1981**, *103*, 7654-7656.

(8) Penner-Hahn, J. E.; McMurry, T. J.; Renner, M.; Latos-Grazynsky, L.; Eble, K. S.; Davis, I. M.; Balch, A. L.; Groves, J. T.; Dawson, J. H.; Hodgson, K. O. *J. Biol. Chem.* **1983**, *258*, 12761-12764.

(9) (a) Terner, J.; Sitter, A. J.; Reczek, C. M. *Biochim. Biophys. Acta* **1985**, *828*, 73-80. (b) Hashimoto, S.; Tatsuno, Y.; Kitagawa, T. *Proc. Jpn. Acad., Ser. B* **1984**, *60*, 345-348. (c) Hashimoto, S.; Tatsuno, Y.; Kitagawa, T. *Proc. Natl. Acad. Sci. U.S.A.* **1986**, *83*, 2417-2421. (d) Sitter, A. J.; Reczek, C. M.; Terner, J. *J. Biol. Chem.* **1985**, *260*, 7515-7522. (e) Hashimoto, S.; Nakajima, R.; Yamazaki, I.; Tatsuno, Y.; Kitagawa, T. *FEBS Lett.* **1986**, *208*, 305-307. (f) Hashimoto, S.; Teraoka, J.; Inubushi, T.; Yonetani, T.; Kitagawa, T. *J. Biol. Chem.* **1986**, *261*, 11110-11118.

0002-7863/90/1512-6809$02.50/0 © 1990 American Chemical Society

PFe^{IV}=O complexes.[10-12] It was also pointed out for horseradish peroxidase compound II that the bound oxygen atom of PFe^{IV}=O is exchanged with that of bulk water only when the bound oxygen atom is hydrogen-bonded to a particular distal residue.[9c] Elucidation of the effective environmental factors that determine the reactivity of PFe^{IV}=O toward oxygenation or oxidation is a topic of current biochemical studies using site-directed mutagenesis.[13a-c]

The autoxidation mechanism of Fe^{II}-porphyrin has been revealed through observation of NMR spectra of the peroxo- ($PFe^{III}OOFe^{III}P$) and oxoferryl intermediates.[14a-d] The reaction is considered to proceed in the following way:

$$PFe^{II} + O_2 \rightarrow PFe^{II}O_2 \ (1) \quad (1)$$

$$2PFe^{II}O_2 \rightarrow PFe^{III}OOFe^{III}P \ (2) + O_2 \quad (2)$$

$$PFe^{III}OOFe^{III}P \rightarrow 2PFe^{IV}{=}O \ (3) \quad (3)$$

$$PFe^{IV}{=}O + H \rightarrow PFe^{III}OH \ (4) \quad (4)$$

$$PFe^{IV}{=}O + PFe^{II} \rightarrow PFe^{III}OFe^{III}P \ (5) \quad (5)$$

Although reaction 5 is a general route, Balch et al.[14c] pointed out from their NMR study that when bulky substituents are bound to the periphery of porphyrin, decomposition of PFe^{IV}=O via eq 5 is unfavorable.

Resonance Raman spectroscopy is a powerful technique for this kind of study since it enables us to detect the Fe^{IV}=O stretching [$\nu(Fe^{IV}{=}O)$], Fe^{II}—O_2 stretching [$\nu(Fe^{II}{-}O_2)$], and O—O stretching [$\nu(O_2)$] vibrations for heme proteins[9a-f] as well as for the corresponding model compounds,[15a,b] allowing discussion about delocalization of electrons among the axial ligand, the iron ion and the porphyrin macrocycle. The $\nu(Fe^{IV}{=}O)$ RR band was first identified for the O_2 matrix of (TPP)Fe^{II} (TPP, tetraphenylporphyrin dianion)[16a,b] and later for low-temperature solutions of (T_{piv}PP)Fe^{IV}=O [T_{piv}PP, *meso*-tetrakis($\alpha,\alpha,\alpha,\alpha$-*o*-pivalamidophenyl)porphyrin dianion][17] and (TMP)Fe^{IV}=O (TMP, 5,10,15,20-tetramesitylporphyrin dianion).[18] Recently, Nakamoto and co-workers observed the $\nu(Fe^{II}{-}O_2)$ and $\nu(O_2)$ RR bands for the O_2 matrix of (TPP)Fe^{II} at 25 K[19] and also the symmetric Fe–O stretching mode of the PFeOOFeP dimer in toluene at −78 °C.[20] On the other hand, we succeeded in simultaneous observation of the $\nu(O_2)$ and $\nu(Fe{-}O_2)$ RR bands for a solution sample of (TMP)$Fe^{II}O_2$ at −100 °C. In this paper we describe the RR spectral change in each step of eqs. 1–4 with a particular emphasis on temperature dependence of intensity of the $\nu(O_2)$, $\nu(Fe^{II}{-}O_2)$, and $\nu(Fe^{IV}{=}O)$ RR bands.

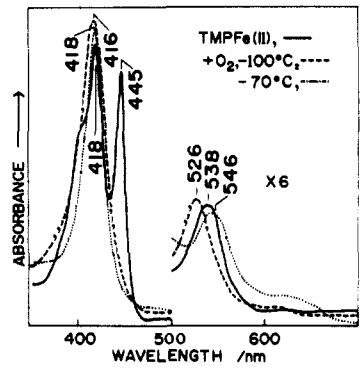

Figure 1. Absorption spectra of (TMP)Fe^{II} and its oxidized intermediates in toluene. Solid line, (TMP)Fe^{II}; broken line, intermediate **1**; dotted line, intermediate **2** (see text).

Experimental Procedures

(TMP)Fe^{III}Cl and its ^{54}Fe-substituted derivative [(TMP)$^{54}Fe^{III}$Cl] were obtained from the reaction of the corresponding ferrous sulfate with $(TMP)H_2$ in *N,N*-dimethylformamide (DMF), followed by the 3 N HCl treatment according to Kobayashi et al.[21] (TMP)Fe^{III}OH was prepared by treatment of (TMP)Fe^{III}Cl with NaOH.[22] Toluene-h_8 (Dojin Chemicals) and toluene-d_8 (Aldrich) were dried with solid sodium and degassed by repeated freeze–pump–thaw cycles. (TMP)Fe^{II} was obtained from sodium mirror contact reduction of (TMP)Fe^{III}Cl in toluene as described previously[23] and confirmed by visible absorption spectra. Autoxidation of (TMP)Fe^{II} was initiated by incorporating O_2 into the toluene solution of (TMP)Fe^{II} at −100 °C, and the subsequent reactions were monitored by visible absorption and NMR spectroscopy. Although the absorption spectra were observed for the 1-mm path length with a known amount of the starting material, we failed to determine the extinction coefficients of individual intermediates, since their precise concentrations were indeterminable.

Raman scattering was excited by the 406.7-nm line of a Kr^+ ion laser (Spectra Physics, Model 264) and detected with a photodiode array (PAR 1420) attached to a Spex 1404 double monochromator. Accumulation time for one measurement was ca. 5 min. Raman shifts were calibrated with indene and accuracy of frequencies of well-defined Raman bands were ±1 cm^{-1}. All Raman measurements were performed with a cuvette with 1-mm path length, with which Raman and absorption spectra were measured for an identical preparation, or a spinning cell (1800 rpm), which can be spun in a cryostat containing cooled ethanol.

Results

Figure 1 illustrates the change of visible absorption spectra for each step of eqs 1 and 2. The sodium mirror contact reduction of (TMP)Fe^{III}Cl in toluene yielded the split Soret bands at 418 and 445 nm and the α band at 538 nm, as shown by the solid line. Since several isosbestic points were observed between this and the spectrum of (TMP)Fe^{III}Cl, this should correspond to the one-electron-reduced state, that is, (TMP)Fe^{II}. This species would have no axial ligand and is therefore considered to adopt the intermediate spin state.[24] The depth of the valley between the two peaks at 418 and 445 nm serves as a diagnostic marker for a good preparation; when coordinating impurities are present, the 445-nm band becomes weaker.

Upon incorporation of O_2 into the (TMP)Fe^{II} solution at −100 °C, the 445-nm band disappeared while the 418- and 538-nm bands were shifted to 416 and 526 nm, respectively, as shown by a broken line in Figure 1. This curve is considered to be the absorption spectrum of **1**, although there has been no report about it. When the temperature of the solution was raised to −70 °C, the absorption spectrum drawn by a dotted line was obtained and its NMR spectrum (not shown) exhibited the characteristic

(10) Boso, B.; Lang, G.; McMurry, T. J.; Groves, T. *J. Chem. Phys.* **1983**, *79*, 1122–1126.
(11) Simonneaux, G.; Scholz, W. F.; Reed, C. A.; Lang, G. *Biochim. Biophys. Acta* **1982**, *716*, 1–7.
(12) Oertling, W. A.; Kean, R. T.; Wever, R.; Babcock, G. T. *J. Am. Chem. Soc.*, in press.
(13) (a) Imai, Y.; Nakamura, M. *Biochem. Biophys. Res. Commun.* **1989**, *158*, 717–722. (b) Atkins, W. M.; Sligar, S. G. *J. Am. Chem. Soc.* **1989**, *111*, 2715–2717. (c) Shimizu, T.; Hirano, K.; Takahashi, M.; Hatano, M.; Fujii-Kuriyama, Y. *Biochemistry* **1988**, *27*, 4138–4141.
(14) (a) Chin, D.-H.; Del Gandio, J.; LaMar, G. N.; Balch, A. L. *J. Am. Chem. Soc.* **1977**, *99*, 5486–5488. (b) Chin, D.-H.; LaMar, G. N.; Balch, A. L. *J. Am. Chem. Soc.* **1980**, *102*, 4344–4350. (c) Balch, A. L.; Chan, Y.-W.; Cheng, R.-J.; LaMar, G. N.; Latos-Grazynski, L.; Renner, M. W. *J. Am. Chem. Soc.* **1984**, *106*, 7779–7785. (d) Balch, A. L.; LaMar, G. N.; Latos-Grazynski, L.; Renner, M. W.; Thanabal, V. *J. Am. Chem. Soc.* **1985**, *107*, 3003–3007.
(15) (a) Kitagawa, T.; Ozaki, Y. *Struct. Bonding* **1987**, *64*, 71–114. (b) Spiro, T. G.; Li, X.-Y. In *Biological Application of Raman Spectroscopy*; Spiro, T. G., Ed.; Wiley, New York, 1988; Chapter 1.
(16) (a) Bajdor, K.; Nakamoto, K. *J. Am. Chem. Soc.* **1984**, *106*, 3045–3046. (b) Proniewicz, L. M.; Bajdor, K.; Nakamoto, K. *J. Phys. Chem.* **1986**, *90*, 1760–1766.
(17) Schappacher, M.; Chottard, G.; Weiss, R. *J. Chem. Soc., Chem. Commun.* **1986**, 93–94.
(18) Hashimoto, S.; Tatsuno, Y.; Kitagawa, T. *Proceedings, 10th International Conference on Raman Spectroscopy*; Peticolas, W. L., Hudson, B., Eds.; University Printing Dept, University of Oregon: Eugene, OR, 1986; pp 1.28–1.29.
(19) Wagner, W.-D.; Paeng, I. R.; Nakamoto, K. *J. Am. Chem. Soc.* **1988**, *110*, 5565–5567.
(20) Paeng, I. R.; Shiwaku, H.; Nakamoto, K. *J. Am. Chem. Soc.* **1988**, *110*, 1995–1996.
(21) Kobayashi, H.; Higuchi, T.; Kaizu, Y.; Osada, H.; Aoki, M. *Bull. Chem. Soc. Jpn.* **1975**, *48*, 3137–3141.
(22) Cheng, R.-J.; Latos-Grazynski, L.; Balch, A. L. *Inorg. Chem.* **1982**, *21*, 2412–2418.
(23) Teraoka, J.; Hashimoto, S.; Sugimoto, H.; Mori, M.; Kitagawa, T. *J. Am. Chem. Soc.* **1987**, *109*, 180–184.
(24) (a) Kobayashi, H.; Yanagawa, Y. *Bull. Chem. Soc. Jpn.* **1972**, *45*, 450–456. (b) Collman, J. P.; Hoard, J. L.; Kim, N.; Lang, G.; Reed, C. A. *J. Am. Chem. Soc.* **1975**, *97*, 2676–2681. (c) Kitagawa, T.; Teraoka, J. *Chem. Phys. Lett.* **1979**, *63*, 443–446.

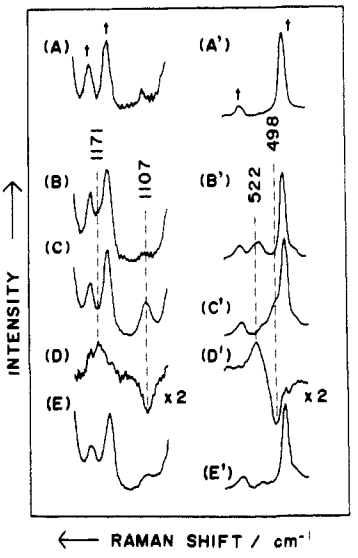

Figure 2. RR spectra of (TMP)Fe^{II} and its oxidized intermediates in the $\nu(O_2)$ (left) and $\nu(Fe^{II}-O_2)$ (right) stretching regions. (A) and (A') (TMP)Fe^{II}; (B) and (B') intermediate **1** obtained with $^{16}O_2$; (C) and (C') intermediate **1** obtained with $^{18}O_2$; (D) difference spectrum [=(B) − (C)]; (D') difference spectrum [=(B') − (C')]; (E) intermediate from $^{18}O_2$ obtained after the sample used to record spectrum C was warmed; (E') intermediate from $^{16}O_2$ obtained after the sample used to record spectrum B' was warmed. The spectra in the $\nu(O_2)$ and $\nu(Fe^{II}-O_2)$ regions were obtained for toluene-h_8 and -d_8 solutions, respectively. Daggers denote Raman bands of solvent.

features of the μ-peroxo dimer reported.[14c] Therefore, the dotted curve is inferred to be the absorption spectrum of **2** with a purity higher than 95%. When the same experiments were carried out with (TPP)Fe^{III}Cl, incorporation of O_2 at −100 °C immediately yielded the spectrum similar to the dotted curve, indicating instability of the $Fe^{II}O_2$ structure in the absence of protecting groups such as methyl groups.

Figure 2 shows the RR spectra in the $\nu(O_2)$ and $\nu(Fe-O_2)$ regions of (TMP)Fe^{II} and **1** in toluene at −100 °C. As shown by spectra A and A', (TMP)Fe^{II} exhibits no prominent RR band in these frequency regions. When $^{16}O_2$ was incorporated into the cell, a trough between two solvent bands at 1158 and 1179 cm^{-1} became noticeably shallow (B) and in addition a new band appeared at 522 cm^{-1} (B'). On the other hand, when $^{18}O_2$ was incorporated, the trough between the two solvent bands remained unchanged compared with spectrum A but a new band appeared at 1107 cm^{-1} (C) and a shoulder appeared at 498 cm^{-1} (C'). The difference spectra between the $^{16}O_2$ and $^{18}O_2$ derivatives, which are shown by traces D [=(B) − (C)] and D' [=(B') − (C')], clearly indicate that the 1171- and 522-cm^{-1} bands of the $^{16}O_2$ derivative are shifted to 1107 and 498 cm^{-1}, respectively, for the $^{18}O_2$ derivative. The magnitude of the observed isotopic frequency shifts (64 and 24 cm^{-1}, respectively) are in reasonable agreement with the expected values for the $\nu(O_2)$ ($\Delta\nu$ = 67 cm^{-1}) and $\nu(Fe-O_2)$ ($\Delta\nu$ = 19 cm^{-1}) modes in the diatomic harmonic approximation. Consequently the RR bands of the $^{16}O_2$ derivative of **1** at 1171 and 522 cm^{-1} are assigned to the O–O and Fe–O_2 stretching vibrations, respectively. This is the first simultaneous observation of the $\nu(O_2)$ and $\nu(Fe-O_2)$ modes for $PFe^{II}O_2$ in solution and strongly supports the idea that the solid line in Figure 1 stands for the absorption spectrum of **1**. Spectra E and E' in Figure 2 show the RR spectra of the $^{18}O_2$ and $^{16}O_2$ derivatives at −70 °C, respectively, which were observed for the same samples as used for obtaining spectra C and B' respectively. The $\nu(O_2)$ and ν-$(Fe-O_2)$ RR bands disappear upon warming to −70 °C.

Figure 3 shows the RR spectrum of **1** in toluene-d_8 at −100 (A) and −70 °C (B and C). The RR bands of **1** at 1569 and 1367 cm^{-1} are assignable to the ν_2 and ν_4 mode, respectively.[25] The

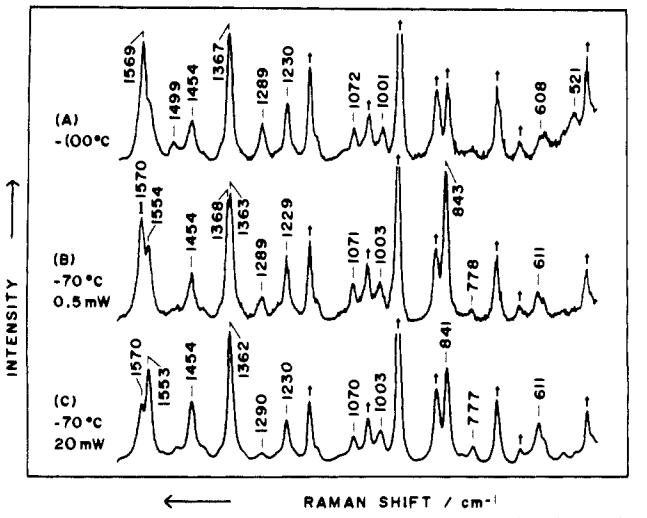

Figure 3. RR spectra of the intermediates **1** and **2** + **3** + **4** in toluene-d_8. (A) Intermediate **1** observed at −100 °C; (B) intermediates **2** + **3** + **4** observed at −70 °C with minimum laser power (0.5 mW at the sample point); (C) intermediates **3** + **4** observed at −70 °C with a higher laser power (20 mW at the sample point). Daggers denote Raman bands of solvent.

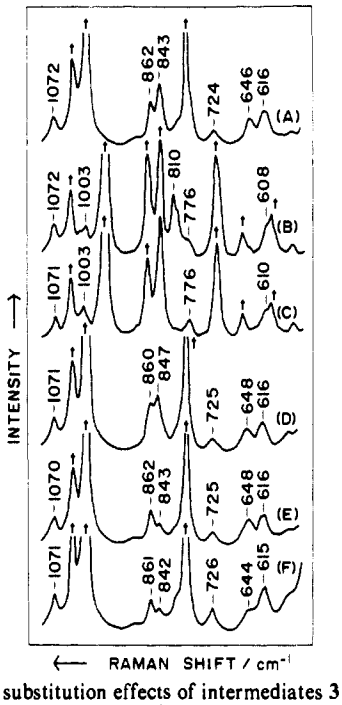

Figure 4. Isotopic substitution effects of intermediates **3** on RR spectra in the 1100–550-cm^{-1} region. (A) ^{16}O derivative in toluene-h_8; (B) ^{18}O derivative in toluene-d_8; (C) ^{16}O derivative in toluene-d_8; (D) ^{54}Fe, ^{16}O derivative in toluene-h_8; (E) ^{16}O derivative after being warmed to −30 °C and cooled to −70 °C in toluene-h_8; (F) (TMP)Fe^{III}OH in toluene-h_8. Daggers denote Raman bands of solvent.

ν_4 frequency of **1** is higher than that of (TMP)Fe^{III}Cl (1364 cm^{-1}) in consonance with the results for hemeproteins such as Hb and Mb for which the ν_4 frequency is higher for the oxy form than for the met form.[26,27] When the temperature of the solution was raised to −70 °C and its RR spectrum was measured with very low laser power, a new band was recognized at 843 cm^{-1} as shown by spectrum B. When the laser power was raised to 20 mW without changing the temperature of the sample, the bands at 1570, 1368, and 843 cm^{-1} became weaker. Although these measurements were performed with the cuvette, the same results

(25) Li, X.-Y.; Czernuszewicz, R. S.; Kincaid, J. R.; Su, Y. O.; Spiro, T. G. *J. Phys. Chem.* **1990**, *94*, 31–47.

(26) Spiro, T. G.; Strekas, T. C. *J. Am. Chem. Soc.* **1974**, *96*, 338–345.
(27) (a) Kitagawa, T.; Iizuka, T.; Saito, M.; Kyogoku, Y. *Chem. Lett.* **1975**, 849–852. (b) Kitagawa, T.; Kyogoku, Y.; Iizuka, T.; Ikeda-Saito, M. *J. Am. Chem. Soc.* **1976**, *98*, 5169–5173.

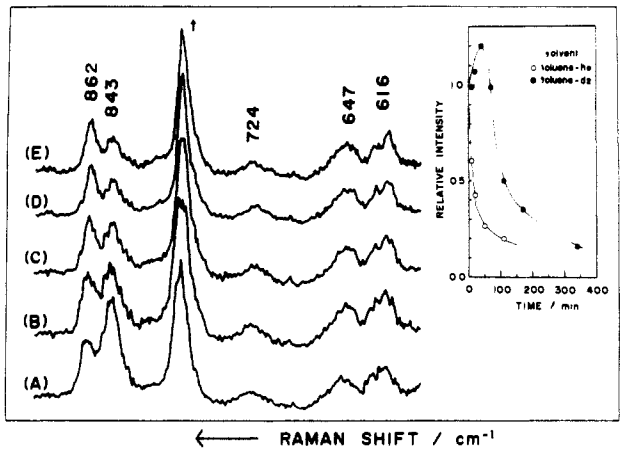

Figure 5. Intensity change of the $\nu(Fe^{IV}=O)$ RR band due to thermal decomposition of **3**. Spectrum A was observed in toluene-h_8 at −70 °C just after preparation at −100 °C, whereas spectra B–E were observed at −100 °C after the sample was kept at −30 °C for 10, 20, 50, and 110 min, respectively. The inset shows the relative intensity of the $\nu(Fe^{IV}=O)$ RR band to the solvent band (at 783 cm^{-1} for toluene-h_8 and at 869 cm^{-1} for toluene-d_8) plotted against the period in which the sample was kept at −30 °C; A dagger denotes the solvent band used as reference.

were obtained with the spinning cell. In order to understand the implication of these spectral changes, the RR spectra in the 1000–600-cm^{-1} region were examined in detail.

Spectra A and B in Figure 4 were obtained at −70 °C for the $^{16}O_2$ derivative in toluene-h_8 and the $^{18}O_2$ derivative in toluene-d_8, respectively. A new band appeared at 810 cm^{-1} in spectrum B. When $^{16}O_2$ was used in toluene-d_8, the 810-cm^{-1} band disappeared and the band at 843 cm^{-1} was relatively intensified as shown by spectrum C, indicating that a solute band was overlapped with a solvent band at 841 cm^{-1}. Accordingly, the 843- and 810-cm^{-1} bands should be associated with vibrations involving motions of ^{16}O and ^{18}O, respectively. If the species observed were **2**, the oxygen isotope sensitive band would be the O–O stretching mode of the peroxo-bridged dimer, and if the species observed were **3**, it would be the $\nu(Fe^{IV}=O)$ mode. To determine the alternative, the same experiment was carried out for the ^{54}Fe derivative, and the results are shown by spectrum D. Comparison of spectrum D with spectrum A indicates that the 843-cm^{-1} mode is ^{54}Fe isotope sensitive and therefore should significantly involve the Fe–O stretching character. The magnitudes of the observed frequency shifts (33 cm^{-1} for $^{16}O/^{18}O$ and 4 cm^{-1} for $^{56}Fe/^{54}Fe$) are closer to those expected for a Fe–O diatomic oscillator ($\Delta\nu$ = 37 cm^{-1} for $^{16}O/^{18}O$ and 3.4 cm^{-1} for $^{56}Fe/^{54}Fe$) than that for an O–O diatomic oscillator ($\Delta\nu$ = 48 cm^{-1}). Furthermore, the observed shifts are in good agreement with the corresponding data for the five-coordinate $Fe^{IV}=O$ porphyrin obtained in an O_2 matrix at 15 K ($\Delta\nu$ = 34 cm^{-1} for $^{16}O/^{18}O$ and 4 cm^{-1} for $^{56}Fe/^{54}Fe$).[16a,b] Consequently, we assign the 843-cm^{-1} band to the $\nu(Fe^{IV}=O)$ mode and the spectrum shown in Figure 3B to the $Fe^{IV}=O$ complex (**3**) rather than to the PFeOOFeP dimer **2**, contrary to the fact that Balch et al.[14c] assigned the complex at −70 °C to **2**. It seems to be most likely that **2** is extremely photolabile and is immediately converted to **3** when the sample is brought into the laser beam. Probably, the absorption spectrum at −70 °C in Figure 1 reflects **2** but the RR spectrum at −70 °C primarily reflects **3**. Since the laser power dependence of the intensity of the bands at 1570 and 1368 cm^{-1} (Figure 3B) was nearly parallel with that of the 843-cm^{-1} band, they are assigned to the ν_2 and ν_4 modes of **3**, respectively. The ν_2 and ν_4 frequencies of **3** are apparently very close to those of the $Fe^{II}O_2$ complex, but when spectrum C was subtracted from spectrum B, the ν_4 band appeared at 1371 cm^{-1}, which is slightly higher than that of **2** and distinctly higher than that of the Fe^{III}–OH complex (vide infra).

When the temperature of the sample used for the measurement of spectrum A in Figure 4 was raised to −30 °C and cooled to −70 °C again, spectrum E was obtained. This spectrum is practically the same as the spectrum of authentic (TMP)Fe^{III}OH shown by spectrum F. It implies that (TMP)$Fe^{IV}=O$ is reduced to (TMP)Fe^{III}OH at −30 °C according to eq 4, in agreement with the results from NMR studies.[14a-c] The spectral change from Figure 4A to E was pursued in detail and the results are illustrated in Figure 5.

Table I. Oxygen–Oxygen and Iron–Oxygen Stretching Frequencies of Oxy Ferrous Porphyrins

compound[a]	$\nu(O_2)$, cm^{-1}	$\nu(Fe-O_2)$, cm^{-1}	temp, °C	ref
Fe(TMP)O_2	1171	522	−100	this work
Fe(TPP)O_2				
end-on	1195	509	−248	19
side-on	1106		−258	30a
Fe(OEP)O_2				
end-on	1190		−258	30a
side-on	1104		−258	30a
Fe(T_{piv}PP)(1-MeIm)O_2	1159	571	RT[b]	31, 32
Fe(TPP)(Pip)O_2	1157	575	−70	30b

[a] Abbreviations: TPP, tetraphenylporphyrin; OEP, octaethylporphyrin; T_{piv}PP, *meso*-tetrakis($\alpha,\alpha,\alpha,\alpha$-*o*-pivalamidophenyl)porphyrin; Im, imidazole; Pip, piperidine. [b] RT, room temperature.

Spectrum A in Figure 5 was observed for (TMP)$Fe^{IV}=O$ in toluene-h_8 at −70 °C. When the sample was kept at −30 °C for 10, 20, 50, and 110 min, spectra B–E, respectively, were observed. The 843-cm^{-1} bands became weaker with lapse of time. The inset of Figure 5 displays the plot of the relative intensity of the 843-cm^{-1} band to a solvent band vs the period kept at −30 °C. The open and closed circles denote the data obtained from the toluene-h_8 and -d_8 solutions, respectively. The ordinate is scaled with regard to the value at 0 min of each series.

The increase of intensity during the initial 50 min with the toluene-d_8 solution means an increase in **3**. Since the formation of **3** from **2** runs in parallel with the reduction of **3** to **4**, the accumulation of **3** can be recognized when the latter reaction is relatively slower. In fact, such a feature can be simulated when the formation and decay rates of **3** are of similar magnitude. Consequently, the results shown in the inset of Figure 5 imply that the decay of the $Fe^{IV}=O$ species is faster in toluene-h_8 than in toluene-d_8. This is consistent with the recent report that the oxoferryl porphyrin π cation radical, whose reduction to neutral oxoferryl porphyrin is considered to involve hydrogen abstraction from solvent, is more stable in CD_2Cl_2 than in CH_2Cl_2.[28]

We note that the RR spectrum finally obtained at −30 °C (Figure 5E) is coincident with the spectrum obtained at −70 °C with a higher laser power (not shown, but the corresponding spectrum in toluene-d_8 is shown by Figure 3C). This means that reduction from **3** to **4** is also promoted by laser illumination. Therefore, it is quite important to use a lower laser power to observe RR spectra of the peroxo-bridged and oxoferryl porphyrins.

Discussion

In the ^1H NMR study on autoxidation of (TMP)Fe^{II} by Balch et al.,[14c] the first intermediate observed upon incorporation of O_2 to (TMP)Fe^{II} was the peroxo-bridged dimer, although O_2 was incorporated at −70 °C and the presence of some precursor was anticipated. The observation of $\nu(O_2)$ in the present study demonstrated that the first intermediate is the Fe^{II}–O_2-type complex and relatively photostable. The NMR study with more sterically crowded porphyrins[29] also yielded evidence for the formation of diamagnetic PFe^{II}–O_2 complex at −70 °C as the primary compound. The $\nu(O_2)$ and $\nu(Fe^{II}-O_2)$ vibrations of oxygenated iron porphyrins have been investigated by several groups and their results are summarized in Table I. The $\nu(O_2)$ mode has been detected only by IR spectroscopy[30a,b,31] for the oxy form of iron

(28) Gold, A.; Joyaraj, K.; Doppelt, P.; Weiss, R.; Chottard, G.; Bill, E.; Ding, X.; Trautwein, A. X. *J. Am. Chem. Soc.* **1988**, *110*, 5756–5761.
(29) Latos-Grazynski, L.; Cheng, R.-J.; La Mar, G. N.; Balch, A. L. *J. Am. Chem. Soc.* **1982**, *104*, 5992–6000.
(30) (a) Watanabe, T.; Ama, T.; Nakamoto, K. *J. Phys. Chem.* **1984**, *88*, 440–445. (b) Nakamoto, K.; Paeng, I. R.; Kuroi, T.; Isobe, T.; Oshio, H. *J. Mol. Struct.* **1988**, *189*, 293–300.

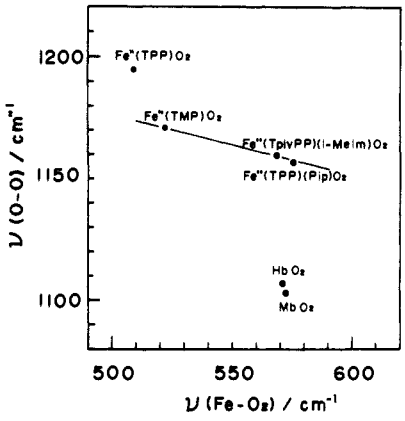

Figure 6. The $\nu(O_2)$ vs $\nu(Fe^{II}–O_2)$ plot for oxygenated iron porphyrins and heme proteins. $Fe^{II}(TPP)O_2$, data from refs 30a (IR) and 19 (Raman); $Fe^{II}(TPP)(Pip)O_2$, data from ref 30b; $Fe^{II}(T_{piv}PP)(1\text{-MeIm})O_2$, data from refs 32 (IR) and 31 (Raman). The straight line represents $\nu(O_2) = -0.264\nu(Fe^{II}–O_2) + 1309$ (see text).

porphyrins and heme proteins[15a] until recently Wagner et al.[19] succeeded in observing the $\nu(O_2)$ and $\nu(Fe^{II}–O_2)$ RR bands for $(TPP)Fe^{II}O_2$ in a dioxygen matrix at 25 K. The present experiment also provided the first simultaneous observation of the $\nu(O_2)$ and $\nu(Fe^{II}–O_2)$ RR bands for a solution state. Since the $\nu(O_2)$ frequency for the side-on geometry is distinctly low,[30a] the present $\nu(O_2)$ frequency suggests that the O_2 molecule in **1** adopts the end-on geometry.

The $\nu(O_2)$ frequencies are plotted against $\nu(Fe^{II}–O_2)$ frequencies in Figure 6. The $\nu(Fe–O_2)$ frequencies are higher for six-coordinate complexes than for the five-coordinate complexes,[12,17,18,30a,b,32] in contrast with the $\nu(Fe^{IV}=O)$ frequencies of the $Fe^{IV}=O$ porphyrins. The $\nu(O_2)$ frequencies become lower as $\nu(Fe^{II}–O_2)$ frequencies become higher in consonance with the relation of $\nu(CO)$ vs $\nu(Fe^{II}–CO)$.[33] The data from solutions fall on a straight line drawn in Figure 6, which is represented by

$$\nu(O_2) = -0.264\nu(Fe^{II}–O_2) + 1309$$

but those from $(TPP)Fe^{II}O_2$ in a dioxygen matrix at 25 K[19] and proteins deviate significantly from the line. One may argue against this to point out that $(TPP)Fe^{II}O_2$, $(TMP)Fe^{II}O_2$, HbO_2, and MbO_2 form a straight line and that the six-coordinate porphyrins in the solution fall off the line. If such line were drawn, it would be given by

$$\nu(O_2) = -1.306\nu(Fe^{II}–O_2) + 1853$$

For the limit of $\nu(Fe^{II}–O_2) = 0$ cm^{-1}, the extrapolated $\nu(O_2)$ frequency with the former equation is closer to the gas-phase value (1551 cm^{-1}, it would be lower than this in an aqueous solution) than that with the latter equation. Furthermore, when we think about some regularity between the two kinds of frequencies, it is more reasonable to contain all solution data in a group rather than to involve the data from the solid matrix at 25 K at the expense of a part of the solution data.

The deviations of the protein data from the straight line shown in Figure 6 imply that π back-donation from $d_{yz}(Fe)$ and $d_{xz}(Fe)$ orbitals, which leads to lowering of the $\nu(O_2)$ frequency and to raising of the $\nu(Fe^{II}–O_2)$ frequency, is sensitively affected by surroundings or that the $\nu(O_2)$ frequency is very sensitive to interactions of bound O_2 with distal residues in the protein as suggested by Oertling et al.[12] The difference in π back-donation would alter polarization of the $Fe^{II}–O_2$ bond and thus the reactivity of oxygen. Another possibility is that the hydrogen bonding between O_2 and protein residues little alters the $\nu(O_2)$ and $\nu(Fe^{II}–O_2)$ frequencies but changes the Fe–O–O bond angle, which results in a large change of $\nu(O_2)$ and $\nu(Fe^{II}–O_2)$ frequencies. The compounds that fall off the straight line in Figure 6 may have different Fe–O–O bond angles.

It is fairly certain that the absorption spectrum obtained at −70 °C (Figure 1) reflects **2**, since the ^1H NMR spectrum reproduced that of **2** reported[14c] and the amount of impurity like **3** is deduced to be less than 5%. The absorption spectral changes in reactions 1–3 were reported by Paeng et al.[20] The relative absorbances at 418 and 445 nm of $(TMP)Fe^{II}$ are significantly different between the reported (Figure 2A in ref 20) and the solid line in Figure 1, and the reported curve could be reproduced when reduction by the sodium mirror was incomplete and/or the solution was contaminated by an impurity. Paeng et al.[20] observed an oxygen isotope sensitive band at 574 cm^{-1} upon incorporation of $^{16}O_2$ to $(TMP)Fe^{II}$ at −78 °C and assigned it to the symmetric Fe–O stretching mode of the FeOOFe dimer. Although we failed to detect the 574-cm^{-1} band, we expected to recognize it in the spectra shown in Figure 2, if present. Presumably the peroxo-bridged dimer is a poor Raman scatterer at this excitation wavelength and undergoes rapid homolytic cleavage upon laser illumination, leading to formation of the oxoferryl complex, while the rate-limiting step in reduction of oxoferryl complex is the hydrogen abstraction from solvent molecules.

The reported absorption spectrum (Figure 2B in ref 20) is also different from any in Figure 1. Therefore, the interpretation by Paeng et al.[20] might be correct, but judging from their absorption spectrum of PFe^{II} we cannot rule out a possibility that the 574-cm^{-1} band arised from a six-coordinate $PFe^{II}O_2$. However, in this case, it is puzzling why upon warming to −46 °C the $\nu(Fe^{IV}=O)$ band appeared at 845 cm^{-1}, namely, in the frequency region of the five-coordinate $PFe^{IV}=O$ complexes.

Judging from the $\nu(Fe^{IV}=O)$ frequency and chemical species coexistent in the solution, **3** in this experiment is considered to adopt the five-coordinate structure. The $\nu(Fe^{IV}=O)$ frequency of the five-coordinate $(TPP)Fe^{IV}=O$ in a dioxygen matrix at 15 K (852 cm^{-1})[16a] is slightly higher than the present value. This would not be due to a difference in the type of porphyrin, because the $\nu(Fe^{IV}=O)$ frequencies of $(TPP)Fe^{IV}=O$, $(OEP)Fe^{IV}=O$, and $(salen)Fe^{IV}=O$ [salen, *N,N'*-ethylenebis(salicylideneiminato)] in a dioxygen matrix are the same.[16b] The $\nu(Fe^{IV}=O)$ frequency is expected to become lower for six-coordinate complexes (841–807 cm^{-1})[12] than for five-coordinate complexes (852–843 cm^{-1}) due to σ donation from a trans ligand to the antibonding orbital of the $Fe^{IV}=O$ bond.[12,34] The $\nu(Fe^{IV}=O)$ frequencies reported for heme proteins (797–767 cm^{-1}) are still lower than those of the six-coordinate $PFe^{IV}=O$ complexes, presumably due to hydrogen bonding to a distal residue and/or protein effects on bond polarization.

It is quite important to establish the RR spectrum of **3** for comparison with that of oxoferryl porphyrin π cation radical in future. Spectrum B in Figure 3 contained appreciable contribution from **4** and we failed to isolate **3**. On the basis of the parallel behavior of intensities among the bands at 1570, 1368, and 843 cm^{-1}, we assigned the 1570-, and 1368-cm^{-1} bands to ν_2 and ν_4 of $(TMP)Fe^{IV}=O$. The first two bands have not been reported yet for this complex, while the $\nu(Fe^{IV}=O)$ frequency is in agreement with that reported.[20]

The reduction mechanism of **3** to **4** has not been discussed in the previous NMR study.[14c] The great difference in the reduction rate between the toluene-h_8 and -d_8 solutions, which was noticed in this study for the first time, evidently indicated that a reductant is solvent toluene and the hydrogen (or deuterium) abstraction brings about a mass effect of the transferred reducing equivalent on the reaction from **3** to **4**.

The chemistry of the oxoferryl porphyrin has been extensively investigated in relation to intermediates of oxygenation reactions by cytochrome P-450.[2a,b] Presumably, the oxoferryl oxygen has an appreciable radical character, which leads to the hydrogen abstraction by **3**, and the radical character of the $Fe^{IV}=O$ bond

(31) Collman, J. P.; Brauman, J. I.; Halbert, T. R.; Suslick, K. S. *Proc. Natl. Acad. Sci. U.S.A.* **1976**, *73*, 3333–3337.
(32) Kerr, E. A.; Mackin, H. C.; Yu, N.-T. *Biochemistry* **1983**, *22*, 4373–4379.
(33) Li, X. Y.; Spiro, T. G. *J. Am. Chem. Soc.* **1988**, *110*, 6024–6033.
(34) Su, Y. O.; Czernuszewicz, R. S.; Miller, L. A.; Spiro, T. G. *J. Am. Chem. Soc.* **1988**, *110*, 4150–4157.

is promoted by electronic excitation. Therefore, the reaction from **3** to **4** seemed to be accelerated by laser illumination as well as by thermal excitation.

In conclusion, resonance Raman spectra for autoxidation intermediates of ferrous porphyrin were obtained and they are consistent with eqs 1–4 deduced from NMR spectroscopy.[14c] Some additional new information obtained here demonstrated the presence of the Fe^{II}—O_2 complex at −100 °C and the Fe^{IV}=O complex at −70 °C, although they are photolabile, and suggested that reduction of the Fe^{IV}=O porphyrin proceeds via hydrogen abstraction from solvent (toluene).

Acknowledgment. This work was partly supported by Grant-in-Aids for Scientific Research in Priority Area to T.K. (63635005) and to Y.T. (62607516) from the Ministry of Education, Science, and Culture.

(Tetrakis(2-pyridylmethyl)ethylenediamine)iron(II) Perchlorate, the First Rapidly Interconverting Ferrous Spin-Crossover Complex

Hsiu-Rong Chang,[1] James K. McCusker,[1,2] Hans Toftlund,*[,3] Scott R. Wilson,[1] Alfred X. Trautwein,[4] Heiner Winkler,[4] and David N. Hendrickson*[,2]

Contribution from the School of Chemical Sciences, University of Illinois, Urbana, Illinois 61801, Department of Chemistry, D-0506, University of California at San Diego, La Jolla, California 92093-0506, Department of Chemistry, University of Odense, DK-5230 Odense M, Denmark, and Department of Physics, Medizinische Universitat, 2400 Lübeck 1, West Germany.
Received November 20, 1989. Revised Manuscript Received March 20, 1990

Abstract: The preparation and characterization of the first Fe^{II} spin-crossover complex that interconverts between high- and low-spin states at a rate faster than the ^{57}Fe Mössbauer time scale is reported. $[Fe(tpen)](ClO_4)_2 \cdot {}^2/_3H_2O$ crystallizes in the monoclinic space group $C2/c$, which at 298 K has a unit cell of a = 40.87 (2) Å, b = 9.497 (4) Å, c = 23.946 (9) Å, and β = 108.42 (4)° with Z = 12 and at 358 K the unit cell is characterized by a = 41.00 (2) Å, b = 9.517 (5) Å, c = 24.21 (1) Å, and β = 109.46 (4)° with Z = 12. The hexadentate ligand tpen is tetrakis(2-pyridylmethyl)ethylenediamine. The refinements were carried out with 3110 (2.58σ) and 2221 (2.58σ) observed reflections at 298 and 358 K, respectively, to give R = 0.073 and R_w = 0.076 at 298 K and R = 0.082 and R_w = 0.082 at 358 K. At both temperatures there are two crystallographically different $[Fe(tpen)]^{2+}$ cations. One of these two cation sites has a greater high-spin content, as evidenced by Fe–ligand atom bond lengths and trigonal distortions which are greater than those found at the other cation site. The Fe–N bond lengths and trigonal distortion increase for both cations as the temperature is increased from 298 to 358 K. Solid-state magnetic susceptibility data show that the critical temperature, T_c, where there are equal amounts of high- and low-spin complexes, is T_c = 365 K. Faraday balance data for this same perchlorate salt in DMF solution give T_c = 363 K. The similarity of these solid- and solution-state T_c values and the susceptibility data taken for the pure solid and solid solutions in the isostructural Zn^{2+} complex definitively show that the spin-crossover cations in $[Fe(tpen)](ClO_4)_2 \cdot {}^2/_3H_2O$ experience no appreciable intermolecular interactions. Each cation acts independently in a high-/low-spin equilibrium. The ^{57}Fe Mössbauer spectrum exhibits only one quadrupole-split doublet for each cation up to the highest temperature (350 K) investigated. Thus, this is the first Fe^{II} spin-crossover complex that interconverts in the solid state between high- and low-spin states at a rate that is faster than the Mössbauer time scale. A careful analysis of the changes in the structure of the $[Fe(tpen)]^{2+}$ cation as a function of temperature together with angular overlap calculations suggest that it is the increase in Fe–N bond lengths together with an increase in the trigonal distortion that leads to the fast rate of spin-state interconversion in $[Fe(tpen)]^{2+}$. The steric constraints introduced by the hexadentate ligand lead to a relatively large trigonal distortion lowering the energy of triplet excited states ($^3T_1$ and/or $^3T_2$). This then leads to greater spin–orbit interaction of the ^1A low-spin state with components of the $^5T_2$ high-spin state, and a greater rate of interconversion results. Additional evidence supporting the presence of fluxional distortions of $[Fe(tpen)]^{2+}$ along a trigonal twisting coordinate is presented in the form of variable-temperature ^1H NMR data. In solution $[Fe(tpen)]^{2+}$ exhibits a very fast rate (>600 s^{-1}) of enantiomerization. Finally, the preparation and properties (T_c > 400 K) of $[Fe(tpen)](ClO_4)_2$ are given. This non-hydrated complex crystallizes in the monoclinic space group $P2_1/c$, which at 298 K has a unit cell characterized by a = 17.865 (3) Å, b = 9.878 (1) Å, c = 17.213 (4) Å, and β = 110.01 (2)° with Z = 4. This structure was refined with 3031 (2.58σ) observed reflections to give R = 0.049 and R_w = 0.053. The trigonal twist found for the cation is in keeping with magnetic susceptibility data indicating that this nonhyrated complex is totally low spin at 298 K.

Introduction

In addition to oxygenation and carbonylation of myoglobin and hemoglobin, electron-transfer reactions of heme proteins are often associated with a change in the spin-state of an iron ion from high spin to low spin and vice versa.[5] For example, there has been considerable interest in the coupling of spin, substrate, and redox equilibria in cytochrome P450.[6] It has been shown that the

(1) University of Illinois.
(2) University of California at San Diego.
(3) University of Odense.
(4) Medizinsche Universitat.

(5) (a) Dose, E. V.; Tweedle, M. F.; Wilson, L. J.; Sutin, N. *J. Am. Chem. Soc.* **1977**, *99*, 3886. (b) Dyson, H. J.; Beattie, J. K. *J. Biol. Chem.* **1982**, *257*, 2267. (c) George, P.; Beetlestone, J.; Griffith, J. S. *Rev. Mod. Phys.* **1964**, *36*, 441. (d) Ogunmola, G. B.; Kauzmann, W.; Zipp, A. *Proc. Natl. Acad. Sci. U.S.A.* **1976**, *73*, 4271. (e) Fisher, M. T.; Sligar, S. G. *Biochemistry* **1987**, *26*, 4797.

(6) (a) Raag, R.; Poulus, T. L. *Biochemistry* **1989**, *28(2)*, 917. (b) Moura, I.; Liu, M. Y.; Costa, C.; Liu, M. C.; Pai, G.; Xavier, A. V.; LeGall, J.; Payne, W. J.; Moura, J. J. G. *Eur. J. Biochem.* **1988**, *177(3)*, 673.

0002-7863/90/1512-6814$02.50/0 © 1990 American Chemical Society